A Quantitative Analysis of Hydrogen Trapping

G. M. PRESSOUYRE AND I. M. BERNSTEIN

The complex hydrogen trapping characteristics of iron-titanium-carbon alloys, containing both reversible and irreversible traps have been fully analyzed. The key to this quantitative analysis is a complete identification of the type and number of each operating trap. The trapping parameters were obtained from an analysis of the relevant hydrogen permeation transients. Titanium substitutional atoms have been shown to be reversible, low occupancy traps with an interaction energy with hydrogen, E (Ti-H), of 0.27 eV. Typical rate constants for these alloys are; a hydrogen capture rate constant of approximately 10^{-24} $cm^3/atom \cdot s$ a release rate constant of approximately 10^{-3} s^{-1}, and a trapping rate of the order of 10^{15} atoms, $H/cm^3 \cdot s$. TiC particles are irreversible traps with a large occupancy and an interaction energy, E (TiC-H), of 0.98 eV. The irreversible trapping parameters are calculated from the first permeation transient, where mixed trapping occurs. The trapping kinetics are about an order of magnitude faster than when only reversible trapping exists. The role of trapping on the effective diffusivity of hydrogen is discussed as is, briefly, its role in affecting hydrogen-induced damage. Finally, guidelines are given to permit the trapping behavior of more general alloys to be analyzed.

SINCE its existence was suggested by Darken and Smith[1] in 1949, hydrogen trapping has been well substantiated, both experimentally and theoretically. Traps that have now been identified in iron and other metals include dislocations,[2,3] grain boundaries,[3,4] voids,[5,6] and particle-matrix interfaces.[3,4,7] The importance of such internal traps on hydrogen diffusion and on determining an alloy's susceptibility towards hydrogen embrittlement is also well documented.[8-10] What is lacking, however, is a reliable technique for not only identifying such traps, but also of predicting what their effect will be. It is usual to attempt to obtain trapping parameters from an analysis of the permeation rate of hydrogen through a material, drawing upon one of several existing theories, the most general being that of McNabb and Foster,[11] in which Fick's first and second laws have been modified to include a trapping reaction. Although the resulting differential equations cannot be solved explicitly, numerical solutions have been proposed in the literature most recently by Caskey and Pillinger.[12] While other theories or models, in particular those of Oriani,[13] Koiwa,[14] and Pressouyre and Bernstein,[15] also treat the same problem they require simplifying assumptions which may or may not apply to all realistic cases.[10] A further problem common to all these models, is that due to their intrinsic generality and the large number of associated parameters,[11] or due to the complexity of the material itself, it is often difficult to distinguish between the trapping characteristics of different traps, thus making it difficult to determine the trapping and release rates, trap efficiency, and the interaction energy between various traps and hydrogen. In this paper we describe an approach from which quantitative trapping parameters can be obtained. The key is the use of a model system in which the trap population is not only known but controllable. In fact, we will be able to analyze a quite complex trapping situation where both reversible and irreversible trapping may occur simultaneously.* Extensions of the present study to even more complex situations, as well as applications towards predicting hydrogen embrittlement susceptibility will also be discussed.

*These trapping terms are defined as follows: a reversible trap is one at which hydrogen has a short residence time at the temperature of interest with an equivalent low interaction energy. On the other hand for the same conditions an irreversible trap is one with a negligible probability of releasing its hydrogen.

I. MATERIALS AND EXPERIMENTAL SET-UP

The base material for this study consisted of pure α-iron to which specific quantities of titanium and carbon were added, but in limited quantities so as to maintain as simple a microstructure as possible. The chemical composition of the alloys is given in Table I. Six alloys were considered, with low, medium, and

Table I. Chemical Composition of the Alloys Used in This Study; ppm are Weight ppm

Alloy	Ti, Wt Pct	Minimum Free Titanium,* Wt Pct	C, ppm	N, ppm	O, ppm
		Ferrovac E			
A	0	–	56	10	18
		Low Ti Content			
B	0.15	0.12	50	22	39
BC	0.09	0	320	–	–
		Medium Ti Content			
C	0.63	0.57	110	30	55
CC	0.50	0.24	650	–	–
		High Ti Content			
D	1.50	1.40	270	30	27
DC	1.38	1.22	390	–	–

*Minimum Free Titanium Content = (wt pct Ti) – (4 wt pct C + 3. 4 wt pct N + 1.5 wt pct O).

G. M. PRESSOUYRE, formerly at Carnegie-Mellon University, Pittsburgh, PA is now Research Scientist, Atomic Energy Commission, Bruyères le Châtel, France. I. M. BERNSTEIN is Professor, Carnegie-Mellon University, Pittsburgh, PA 15213.

Manuscript submitted March 2, 1978.

ISSN 0360-2133/78/1113-1571$00.75/0

high titanium content, each with a carburized counterpart.

As determined by electron microscopy and diffraction,[10] and in agreement with the binary Fe-Ti,[16] and ternary Fe-Ti-C[17] phase diagrams, all microstructures consisted of ferrite with primarily incoherent titanium carbide (TiC) particles* of various size densities, as well as titanium atoms in substitutional positions. The size and densities of all particles have been computed using transmission electron micrographs and standard analytical methods,[18] and the results are plotted on Fig. 1. Some of the alloys were also found to have limited regions containing coherent particles. This somewhat special case will be discussed subsequently.

*Strictly speaking, a few of the particles were actually titanium carbo-nitrides or oxides. For simplicity of description, since carbon was the only interstitial solute varied, all particles will be considered as carbides.

All permeation experiments were carried out using an electrochemical cell originally developed by Devanathan and Stachursky,[19] in which hydrogen is introduced by cathodic charging on one side of a metal membrane while exiting hydrogen is oxidized on the other side. The current necessary for a potentiostat to maintain the oxidizing potential of the exiting hydrogen is a direct measure of the output flux of hydrogen. Both cathodic and anodic solutions were 0.1 N NaOH, and the charging current density was maintained at 0.8 mA/cm^2, a value low enough to prevent any internal damage to the membrane.[10]

Specimens were prepared by hot and cold rolling to a thickness of 7.6×10^{-2} cm, (30 mils), and then were annealed at 800°C in argon; a grain size of about 80 μ was obtained for all alloys. Following heat treatment, the membranes were mechanically and chemically polished to a mirror-like finish, and then plated on both sides with a thin (0.1 μ) layer of palladium. Plating the output side with palladium protected the membrane against dissolution at the hydrogen oxidizing potential; plating the input side ensured similar entry conditions for hydrogen, thus effectively eliminating surface effects, as was demonstrated elsewhere.[10,15]

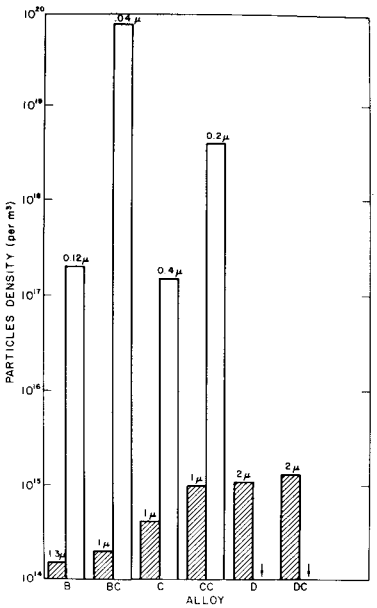

Fig. 1—Density of titanium carbide particles in each alloy. Light bars are for small size particles, dark bars for larger size particles.

II. EXPERIMENTAL RESULTS

Figures 2 and 3 show the effects of titanium additions on the diffusion of hydrogen through ferrite for the noncarburized alloys A, B, C and D, for both the first and second polarization. By the second polarization is meant the subsequent permeation of hydrogen through the membrane after the charging current was turned off following the first polarization, *i.e.*, after the hydrogen flux returned back to zero following which the current was turned back on.

As the titanium content in the iron increases, the permeation becomes slower for all polarizations and for all alloys. Since the decay transients also show the same effect,[10] this slowdown demonstrates both

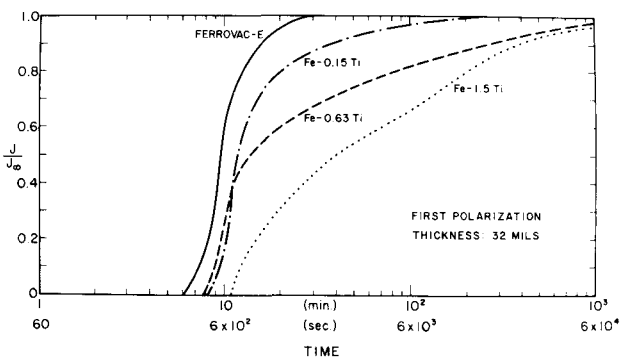

Fig. 2—Normalized output flux of hydrogen *vs* time. First permeation transient.

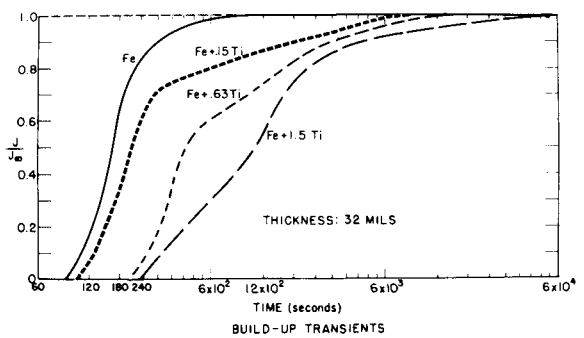

Fig. 3—Normalized output flux of hydrogen *vs* time. Second permeation transient.

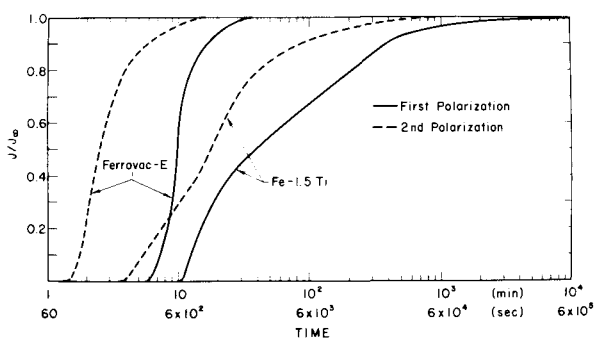

Fig. 4—Comparison of the first and second permeation transients for Ferrovac-E and Fe-1.5Ti. Both reversible and irreversible trapping are present.

the presence of trapping as well as that the traps are directly related to titanium. Moreover, the kind of traps present can be deduced by comparing the successive polarizations of Ferrovac E and alloy D, Fig. 4. This figure clearly shows that in both hydrogen diffuses faster for the second polarization cycle, and that this difference is more marked in alloy D (*i.e.*, when titanium is present). This suggests not only that traps with different degrees of reversibility coexist in the lattice, but that there must also exist irreversible traps which are filled after the first polarization, retain their hydrogen during the first and higher order decay transients, and thus do not contribute to subsequent permeation kinetics.

The above results can be summarized as follows:

a) the first polarization transients give information on the concurrent behavior of irreversible *and* reversible traps,

b) all subsequent polarizations are dominated by the effect of reversible traps,

c) both trapping effects are more pronounced the higher the titanium content.

This last conclusion suggests that the irreversible and reversible traps are related in a direct way to the presence of titanium in the iron matrix. Since "ordinary" traps such as dislocations, grain boundaries, and so forth were found not to vary appreciably in any of the alloys of this study,[10] the extraordinary traps in the titanium bearing alloys are clearly titanium substitutional atoms and titanium carbide particles. Asaoka[4] recently has cathodically charged an alloy identical to our alloy B, and using degassing studies at various temperatures in conjunction with microautoradiography has shown that titanium carbide particles retained hydrogen for much longer times than all other traps. It can thus be initially reasonably assumed that titanium substitutional atoms provide the primary reversible traps, and that TiC particles provide the irreversible traps. The following analyses will demonstrate the validity of this assumption. The approach will be to analyze the second polarization transients first, not only to study reversible trapping, but by difference to yield information on the irreversible trapping parameters deduced from the first polarization transient.

III. ANALYSIS OF REVERSIBLE TRAPPING

A. Theoretical Evidence for an Attraction Between Titanium and Hydrogen

The driving force governing possible trapping of hydrogen by a particular site may have various origins, not all of which are independent of one another. For example, the force can be of chemical (thermodynamical) origin when hydrogen forms a gas (H_2, CH_4) or a hydride (TiH_2), of mechanical origin when hydrogen is subjected to the stress field of a dislocation, or related to the particular electronic state of hydrogen in the lattice. In the particular case of titanium, some of these forces exist, all tending to attract hydrogen to the titanium site, or to neighboring interstitial sites.[10]

a) Thermodynamical Force Between Titanium and Hydrogen. There are several ways of demonstrating the existence of a thermodynamic driving force, the most direct being the sign and amplitude of the first order interaction coefficient between titanium and hydrogen. This term is derived from the definition of the activity coefficient f_i of component i in solution in iron:[20,21]

$$\text{Log } f_i = \sum_j e_i^j \text{ (pct } j\text{)} \qquad [1]$$

Here, j designates every element dissolved in iron (including i), e_i^j = first order interaction coefficient between j and i, and (pct j) = wt pct of j in iron. The importance of e_i^j is that it directly relates the affinity that exists between elements i and j in iron.[21] Indeed, a negative e_i^j is indicative of a thermodynamic attraction between i and j, while a positive e_i^j denotes a thermodynamic repulsion between i and j; the more negative e_i^j, the stronger the attraction, and vice-versa. Although tabulated values of e_i^j are in the literature, these are mainly for elements dissolved in liquid iron.[22-24] However, it has been demonstrated that when these values are corrected to room temperature, the same relative rankings are obeyed.[10,25] Table II illustrates the relative magnitude of certain elements,

Table II. Values of the First Order Interaction Coefficient e_i^H in Liquid Iron at 1600°C

	Attraction $e_i^H < 0$		
Element, i	Reference 22	Reference 23	Reference 24
Ce	–	-0.60	–
Co	–	-0.14	–
Cr	-0.11	-0.33	-0.11
Cu	–	-0.24	–
La	–	-4.3	–
Mn	-0.077	-0.31	-0.077
Mo	–	-0.20	-0.12
Nb	-0.21	-0.61	-0.21
Nd	–	-0.60	–
Ni	0	-0.25	-(0.00)
O	–	-3.10	–
Ta	-3.60	-4.40	-0.23
Ti	-3.85	-1.10	–
V	–	-0.59	-0.24
W	–	–	-0.39
Zr	–	–	-0.13

Table III. Free Energy of Formation of TiH_2 from Free Titanium (*Ti*), Titanium Carbide (TiC) and Titanium Nitride (TiN) in Iron at Room Temperature, for Various Hydrogen and Titanium Contents. The Letters B and D Refer to Table I

Alloy	(Pct H) 5.4×10^{-8}	(Pct H) 1.18×10^{-5}	(Pct H) 0.62×10^{-2}
(*a*) Values of ΔG *(kcal/mole)* for the Reaction: $\underline{Ti}$(pct) + 2$\underline{H}$(pct) = TiH_2(s).			
Fe-0.15Ti (B)	-10.14	-16.57	-23.82
Fe-1.50Ti (D)	-10.83	-17.28	-25.26
(*b*) Values of ΔG (kcal/mole) for the reaction: TiC(s) + 2$\underline{H}$(pct) = TiH_2(s) + $\underline{C}$(pct).			
Fe-0.15Ti	–	9.41	2.08
Fe-1.50Ti	–	-11.24	-18.58
(*c*) Values of ΔG (kcal/mole) for the reaction: TiN(s) + 2$\underline{H}$(pct) = TiH_2(s) + $\underline{N}$(pct).			
Fe-0.15Ti	–	39.35	31.89
Fe-1.50Ti	–	18.68	11.28

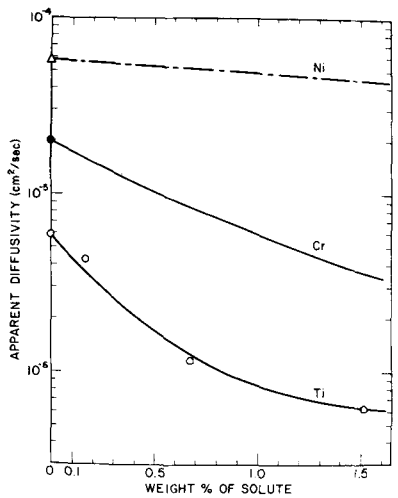

Fig. 5—Variation of the hydrogen diffusivity through ferrite for nickel, chromium and titanium solute additions.

i, that have an attraction for hydrogen in iron; as seen, titanium exhibits one of the most negative first order interaction coefficients, and thus will be one of the most attractive elements for hydrogen.

An upper limit to the thermodynamic driving force existing between elemental titanium dissolved in iron and hydrogen can be obtained by calculating the free energy of formation of the hydride TiH_2 in iron at room temperature obeying the reaction:

$$\underline{Ti} + 2\,\underline{H} \rightleftharpoons TiH_2\ (s) \qquad [2]$$

where Ti = dissolved titanium in iron, H = dissolved monatomic hydrogen in iron, and TiH_2 (s) = precipitated hydride. The calculations are given in Appendix I and in more detail elsewhere;[10] the resultant free energy values are given in Table III, along with similarly obtained values for the possible dissociation of TiC and TiN to form TiH_2. As may be seen, the results confirm the predictions obtained from the interaction coefficient, *i.e.* that there exists a thermodynamic driving force for the formation of TiH_2 at room temperature (since ΔG is negative). The dependence of ΔG on hydrogen content (but not significantly on titanium content) results from considering three possible hydrogen contents, whose magnitude varies with the external hydrogen pressure or fugacity. However, it should be clear that the existence of a driving force does not imply that the reaction will actually take place, nor do we indeed expect a hydride will form. Other considerations of equal or greater importance would be the kinetics of the reaction, any associated strain energy, and so forth. It simply is an indication that there is no thermodynamic barrier to the reaction; further, ΔG is the upper limit of the interaction energy between titanium and hydrogen, E (Ti-H). Finally, Table III also shows that the chemical driving force disappears if titanium is already associated with nitrogen or carbon. Thus the nature of any attraction between TiC and H will not be chemical in origin, in the sense of hydride formation or the tendency to form preprecipitate clusters; instead it will have to be more of a surface adsorption interaction, of a form suggested by the next section.

b) Electronic Force Between Titanium and Hydrogen. There is now considerable evidence[26] that hydrogen dissolves in transition metals by ionizing, *i.e.*, by giving up its electron to the collective electron gas of the metal,[26] thus existing as a screened proton. An interesting feature of this particular state is the effect of impurities. Since hydrogen introduces an excess electron, any impurity that introduces an "electron vacancy" will attract hydrogen to achieve local neutrality. As Friedel states,[27] ". . . one expects hydrogen to be repelled at short range by impurities on the right of the matrix in the periodic table, and attracted by impurities on the left". An examination of the periodic table shows titanium to be located to the left of iron, strongly suggesting an attraction between titanium and hydrogen of electronic origin. In conclusion, strong theoretical support exists for the existence of an attractive force between dissolved titanium and hydrogen in iron. The experimental results will now be analyzed in terms of such an interaction.

B. Analysis of the Diffusivity

The apparent diffusivity, D, in each of the titanium containing alloys has been computed from the second polarization transients, where, as discussed, only reversible trapping operates. The time-lag method was used where the amount of diffusing hydrogen per unit area and unit time, Q_t is calculated as a function of time.[10,19] Q_t is defined as:[28]

$$Q_t = \frac{D\,C_o}{L}\left[t - \frac{L^2}{6D}\right]. \qquad [3]$$

It has been shown by many investigators that the time-lag (at $Q_t = 0$) corresponds to the value of $J/J_\infty = 0.63$, where J and J_∞ are the instantaneous and saturation currents respectively. From this value, the specimen thickness, L, and the input hydrogen concentration, C_o, we can calculate the effective diffusivity. Other techniques exist,[19] but as discussed in depth elsewhere[10] the time-lag method is the most widely used and is considered the most reliable for the present experimental conditions. Time-lag can also be obtained experimentally using an electrical integrator[10] which directly plots Q_t *vs* time. Good agreement was obtained between the results of the two methods. The results for the low-carbon alloys are plotted on Fig. 5, along with similar diffusivity results found in the literature for chromium[29] and nickel[30] additions to iron, also calculated from the time-lag method. As shown in this figure, taking as the diffusivity of hydrogen in nominally pure iron the experimental value for titanium free iron, D exhibits a tenfold decrease with the addition of 1.5 wt pct titanium. The comparison with nickel and chromium is particularly significant, since the decrease in diffusivity with each of these solute additions, D (Fe-i), relative to the diffusivity in the "pure" iron used in each study $D_o(i)$, follows the relative ranking of the respective interaction coefficients (see Table II). This provides further support to the argument that the interaction coefficient is a good measure of the magnitude of the attraction between an element and hydrogen, and thus of hydrogen trapping by a solute element.

McNabb and Foster have developed a rather general theory[11] in which the apparent diffusivity of hydrogen

in iron containing a density of traps N_T, is related to the diffusivity in "pure" iron, D_o, by the relationship:

$$D_o/D = 1 + \frac{k}{p} N_T. \quad [4]$$

In this model it is assumed that D_o corresponds to a situation where no traps exist, $N_T = 0$. This is not strictly true, of course, but the 'background' trap density is insignificant compared for example to when Ti is present; k and p are trapping and release rate parameters defined according to the reaction:

$$dn/dt = kC\ (1 - n) - pn \quad [5]$$

where: n = fraction of traps occupied at time, t; and C = that hydrogen concentration which can diffuse and is thus capable of undergoing a trapping reaction. Equation [4] further assumes that the traps are sparingly occupied; in the particular case of trapping of hydrogen by titanium solute atoms, this has been shown from solubility measurement to be the case,[10] and will be redemonstrated shortly. Other theories[13-15] give a functionally identical expression for D_o/D; these other treatments will be considered in a subsequent section.

Following the original hypothesis that titanium solute atoms are the major internal reversible traps, we now define as a "reversible titanium trap" any of the six octahedral sites nearest to a titanium atom. Thus:

$$N_T = z\, N_{\mathrm{Ti}} \text{ with } 1 < z < 6 \quad [6]$$

where N_{Ti} = density of titanium atoms in the alloy considered.

Accordingly, Eq. [4] predicts:

$$D_o/D = 1 + b\, N_{\mathrm{Ti}}, \quad [7]$$

where now $b = z(k/p)$.

Taking for D_o the experimental value found for Ferrovac E, ($D_o = 6.1 \times 10^{-6}$ cm^2/s), Fig. 5, the ratio D_o/D has been plotted in Fig. 6 as a function of the experimentally known numbers of titanium traps, which for the noncarburized alloys is close to the total titanium content of the alloy. A linear relationship is shown to be obeyed,* supporting the assumption that titanium atoms are the reversible traps responsible for the decrease in diffusivity during second polarization transients.

*The experimental values shown in Fig. 6 represent an average of about forty measurements on each alloy, giving a confidence interval of about 0.5.

By comparing Eqs. [4], [6], and [7], information on the trapping characteristics of titanium atoms can be obtained, in particular, a value for the ratio of the trapping rate parameters:

$$1 \times 10^{-21} < k/p < 6.3 \times 10^{-21}. \quad [8]$$

The ratio of k/p is obviously a function of the number of traps, z, operating per titanium atom. Since all octahedral sites around a titanium atom will not trap with the same efficiency, (*e.g.*, the electronic force decreases as more electrons are brought in by hydrogen atoms), and since we are in a low occupancy case, the real value of k/p is anticipated to be somewhat closer to the lower limit of the inequality,[10] ($z \simeq 1$). The operating assumption that the traps are sparingly occupied can now be verified. At steady state, $dn/dt = 0$ and from Eq. [5]:

$$n_s = \frac{k\,C/p}{1 + k\,C/p}. \quad [9]$$

Hydrogen solubility* and steady state hydrogen flux measurements[10] gave values for C of between 3×10^{17} atoms H/cm^3 (for Ferrovac E) and 12×10^{17} atoms H/cm^3 (for alloy D), predicting that the steady state occupancy, n_s, is always lower than 7.5×10^{-3}. This reinforces the hypothesis that titanium is a low energy, reversible trap of low occupancy. ($z \cong 1$)

*These were obtained using a commercial solid state hydrogen extraction apparatus, manufactured by Leco.

C. Analysis of the Shape of the Transients

A great deal of care must generally be exercised when trying to fit to the McNabb-Foster theory the experimental transients of data like that in Fig. 3, since with the large number of parameters necessary to describe hydrogen trapping, several theoretical curves with widely different sets of permeation parameters could exhibit the same shape. Because of this, any supposed good fit of the experimental curves cannot be said to be unique, and could well be of limited value. In our particular case, however, since N_T, C and the ratio k/p are experimentally known and other parameters have to obey specific relations, this considerably restricts their possible numerical values. To illustrate, let us consider the McNabb-Foster parameters λ, μ, and ν, used by Caskey and Pillinger[12] in their computer study of this theory.[11] These parameters are defined functionally as:

$$\lambda/\mu = b\, N_{\mathrm{Ti}} = kn_t/p \quad [10]$$

$$\lambda/\nu = z\, N_{\mathrm{Ti}}/C = N_t/C. \quad [11]$$

It can be shown[10-12] that λ and ν are related to the

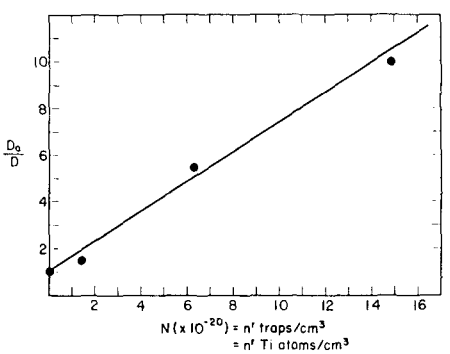

Fig. 6—Experimental verification of a linear relationship between D_o/D and the density of titanium atoms.

Table IV. Experimental Values and Relationships Between Trapping Parameters

Alloy	0.15Ti (B)	0.63Ti (C)	1.50Ti (D)
λ/μ	0.93	3.83	9.30
N_{Ti}(at/cm^3)	1.48×10^{20}	6.22×10^{20}	1.48×10^{21}
C(at/cm^3)	5.6×10^{17}	1.0×10^{18}	1.2×10^{18}
$\lambda/\nu (z = 1)$	2.6×10^{2}	6.2×10^{2}	1.2×10^{3}
$\lambda/\nu (z = 6)$	1.6×10^{3}	3.7×10^{3}	7.2×10^{3}

capture rate constant, k, and μ is related to the release rate constant, p, and further that these parameters are sufficient to almost uniquely determine the permeation curves. In our particular case these ratios are calculable; the results are given in Table IV. These experimental values can be compared with Caskey and Pillinger's[12] tabulated values of the form, λ, μ, and ν, $= 10^{\mp n}$, where n is an integer. For particular sets of λ, μ, and ν, the ratios of the parameters closest to our experimental values, Table IV alloy B, are:

$$\lambda/\mu = 1;\ \lambda/\nu = 100, \text{ if } z = 1 \text{ and } \lambda/\nu = 1000 \text{ if } z = 6$$

and,

$$\lambda = \mu = 1, \text{ for either } \nu = 0.01 \text{ or } \nu = 0.001.$$

Their computer generated theoretical curves derived from these parameters are compared to the experimental curve for alloy B in Fig. 7, for $\nu = 0.01$.

The good fit between theory and experiment is obvious. Unfortunately, for λ and μ much greater than ν, the shape is relatively insensitive to the value of ν so we are not able to infer a value for z, the trapping capacity of an individual Ti atom.

The value of knowing the precise number of traps as well as D_o and C is further illustrated since we can now calculate k and p. From McNabb and Foster:[11]

$$k = \lambda D_o/N_T L^2$$

and [12]

$$p = \mu D_o/L^2$$

where all parameters have their previous meanings. Further, the trapping and release rates in atoms H/s · cm^3 can be obtained from the following relationships (Eq. [5]):

$$\text{trapping rate} = kCN_T\ (1 - n)$$
$$\text{release rate} = pN_T n \qquad [13]$$

where C is taken as the near surface hydrogen concentration, obtainable from steady state results.[10]

Table V illustrates the results of such calculations for alloys B and D. The ratio k/p is equivalent to the value previously calculated using Eq. [7] and Fig. 6. We also find, for alloy B, that with a trapping rate of 5.9×10^{14} atoms H/s · cm^3 and $N_{Ti} = 1.48 \times 10^{20}$ atoms Ti/cm^3, that for any unit of time only 4 Ti atoms/10^6 atoms are actively participating in the trapping reaction, for an occupancy of 7 atoms/10^3 at steady state. These results verify that Ti is a low occupancy, reversible trap, with a low interaction energy.

D. The Interaction Energy Between Titanium and Hydrogen

Although the McNabb-Foster theory does not explicitly yield a value for the interaction energy, E (Ti-H), this term is calculable using Oriani's assumption[13] of dynamic equilibrium between diffusing and trapped hydrogen, a situation well represented by titanium atoms.[10] Following this approach, the equilibrium constant, K, between trapped and diffusing hydrogen is given by:

$$K = \frac{k N_o}{p} \qquad [14]$$

where N_o = number of octahedral diffusion sites in the ferrite bcc lattice = 2.6×10^{23} sites/cm^3.

From Eqs. [8] and [14]:

$$0.26 \times 10^3 < K < 1.6 \times 10^3. \qquad [15]$$

Oriani[13] has proposed that a trapping site is represented by an energy level, ΔE_x, lower than a normal site, but which is itself bounded by an energy barrier $E^1 + E_a$, where E is the normal diffusion activation energy and E^1 represents an additional "step" energy. It therefore follows that:

$$E \text{ (Ti-H)} = E^1 + E_a + \Delta E_x. \qquad [16]$$

Now, $K = \exp(-\Delta E_x/RT)$ and $E_a = 0.08$ eV.[31] Further, we assume that E^1 is of negligible importance but negative in sign,[10,14] following Friedel's argument[27] that this term is likely short range and attractive. Then:

$$0.22 \text{ eV} < E \text{ (Ti-H)} < 0.27 \text{ eV}. \qquad [17]$$

Similar limits have been found by us using somewhat different arguments.[15] Thus, Ti has a trapping strength similar to dislocations and grain boundaries, and well below the value necessary to form an actual hydride, as expected.

IV. ANALYSIS OF IRREVERSIBLE TRAPPING

A. Theoretical Considerations

As previously discussed, any analysis of irreversible trapping in an alloy should be undertaken on the first polarization transient, where these traps are in the process of being irreversibly filled. However, since reversible trapping is simultaneously operating, the analysis must use a compound variable accounting for both types of trapping.

Our results[10] and those of Asaoka[14] support the premise that the dominant irreversible traps are sites at the interface between TiC particles and the

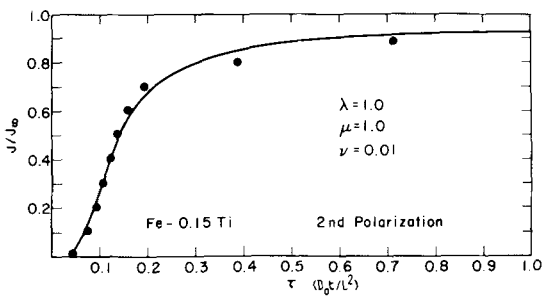

Fig. 7—Fit of the second permeation transient of Alloy B (filled points) with the McNabb-Foster theory (line).

Table V. Trapping Characteristics of Alloys B and D

Alloy	z	λ	μ	ν	k, cm^3/at·s	p, s^{-1}	Trapping Rate, at H/cm^3·s
B	1	1	1	3.8×10^{-3}	7.1×10^{-24}	1.1×10^{-3}	5.9×10^{14}
	6	1	1	6.2×10^{-4}	1.2×10^{-24}	1.1×10^{-3}	5.9×10^{14}
D	1	8.7	0.93	6.2×10^{-4}	6.6×10^{-24}	1×10^{-3}	1.2×10^{16}
	6	8.7	0.93	10×10^{-4}	1.1×10^{-24}	1×10^{-3}	1.2×10^{16}

ferrite matrix. The density of such traps can be given as:

$$N_i = y\,(d)\,N_{\mathrm{TiC}} \qquad [18]$$

where $y\,(d)$ is a function dependent on the size, d, of the particle and N_{TiC} is the density of such particles (Fig. 1). For example, if the particles are spherical we can write for $y\,(d)$:

$$y\,(d) = S\pi\, d^{\,2}/a^2 \qquad [19]$$

where S = number of interstitial sites per unit cell face, d = particle diam, and a = unit cell size.

We now define our compound variable, θ, as:

$$\theta = (n_r + n_i)/(N_r + N_i) \qquad [20]$$

where $n_{r,i}$ = density of hydrogen atoms trapped on reversible and irreversible traps, whose respective densities are $N_{r,i}$.

The total trapping reaction is:

$$d\theta/dt = \overline{k}C\,(1-\theta) - \overline{p}\theta \qquad [21]$$

where $\overline{k}$ and $\overline{p}$ are now the total capture and release rate constants, respectively, for both irreversible and reversible trapping, and C is now the equivalent hydrogen concentration which is either diffusing or is reversibly trapped.

We further define n_{rs} and n_{is} as the saturation values of n_r and n_i at steady state in the first polarization. We have already shown that for low occupancy, $n_{rs} \ll N_r$. From the definition of an irreversible trap $n_{is} = N_i$, *i.e.* all trappable traps are filled. Thus, at steady state:

$$\theta_s = (X N_r + N_i)/(N_r + N_i) \qquad [22]$$

where $X = n_{rs}/N_r$.

Substituting Eq. [22] into Eq. [21],

$$\frac{\overline{k}}{\overline{p}} = \frac{X F_r + F_i}{C(1-x)F_r} \qquad [23]$$

where $F_{r,i} = N_{r,i}/(N_r + N_i)$, the respective fractions of reversible and irreversible traps. Since X, C and F_r are all functions of F_i, $\overline{k}/\overline{p}$ is also a function, albeit a complex one, of F_i, the fraction of irreversible traps. Under conditions where $F_i > X$ and $> F_r$, $\overline{k}/\overline{p}$ would increase proportionally to F_i and thus the effective hydrogen diffusivity would decrease accordingly.

It is possible for our experimental conditions to calculate $\overline{k}/\overline{p}$. We first note that by measurement[10] the hydrogen concentration related to the reversible traps is not different in any significant way between the first and second polarizations. In other words, irreversible trapping has no significant influence on the chemical potential of diffusing and reversibly trapped hydrogen. We can thus substitute for X in Eq. [23] its value when only reversible trapping is present (from Eq. [9]), and obtain after some rearrangement:

$$\frac{\overline{k}}{\overline{p}} = \frac{k}{p}\frac{1}{F_r} + \frac{1}{C}\frac{F_i}{F_r} \qquad [24]$$

(note that in the limit $F_i = 0$, $F_r = 1$ and then $\overline{k}/\overline{p} = k/p$ as expected since there is no irreversible trapping).

In Eq. [24] since $1/F_r > 1$ and since $F_i/C\,F_r > 0$

$$\frac{\overline{k}}{\overline{p}} \geq \frac{k}{p}, \qquad [25]$$

or in other words, irreversible trapping always leads to a greater decrease in diffusivity than reversible trapping.

B. Application of the Theory to Experiment

Figure 8 shows how $\overline{k}/\overline{p}$ varies with F_i/F_r (F_i being obtained from Fig. 1, F_r from the known compositions, and C from hydrogen analysis measurements). The figure predicts that only alloys BC and CC should have a first polarization diffusivity $D(1)$ significantly different than from the second, $D(2)$. In other words:

$$\frac{D(1)\mathrm{BC}}{D(2)\mathrm{BC}} < \frac{D(1)\mathrm{CC}}{D(2)\mathrm{CC}} < \frac{D(1)\mathrm{C}}{D(2)\mathrm{C}}. \qquad [26]$$

Experimental measurements of these diffusivities are shown in Fig. 9 as a function of the Ti content of the alloy. The scatter observed in the carburized alloys is thought to result from a nonuniformity in carbide distribution from one permeation membrane to another.

The inequality predicted by Eq. [2] is found to be obeyed, *i.e.*,

$$0.26\ (\mathrm{BC}) < 0.33\ (\mathrm{CC}) < 0.52\ (\mathrm{C}). \qquad [26]'$$

In the lower carbon alloys (D_2, DC and B) however, the predictions from Fig. 9 are less well obeyed. The likely reasons for this will subsequently be discussed.

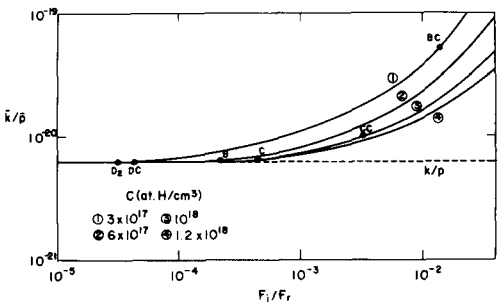

Fig. 8—Variation of trapping rate parameters for first permeation transient with the ratio of irreversible and reversible trapping densities.

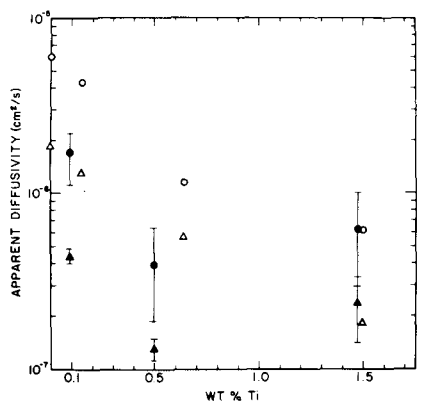

Fig. 9—Hydrogen diffusivity for first (circles) and second (triangles) permeation transients. Light symbols are for uncarburized and dark symbols for carburized alloys.

Table VI. Classification of the Traps Present in Fe-Ti and Fe-Ti-C Alloys Used in This Study

Nature of the Trap	Character of the Trap at Room Temperature	E(Trap-H), eV
Titanium carbide particle (TiC)	Irreversible	0.98 0.8 to 0.98[4]
Grain Boundary	Reversible	0.27[36] 0.55 to 0.61[4]
Dislocation	Reversible	0.25[35]
Titanium substitutional atom	Reversible	0.27
Lattice site	Very reversible diffusion site	0.08[31]

C. Trapping Characteristics of TiC

Since there is as yet no complete theory for combined trapping, independent calculations of $\bar{k}$ and $\bar{p}$ are not possible. However, by reasonably assuming that $\bar{p} = p$ (since detrapping only occurs with reversible traps), we find:

$$\bar{k}_{BC} = 5.3 \times 10^{-23} \text{ cm}^3/\text{atom} \cdot \text{s}$$

compared to

$$k_B = 7 \times 10^{-24} \text{ cm}^3/\text{atom} \cdot \text{s} \qquad \text{(Table V)}.$$

In other words, the addition of carbon to this Fe-Ti alloy increases the trapping kinetics by 7.5 times.

To calculate an interaction energy between TiC and H, an equilibrium approach such as that of Oriani[13] cannot be used since, as discussed,[10] no equilibrium need exist between diffusing and irreversibly trapped hydrogen. However, we have used an electrical analogy model to describe permeation,[10,15] from which we were able to estimate that E (TiC-H) $\simeq$ 0.98 eV. This high value, compared to Ti, agrees with the value found by Asaoka using autoradiography and high temperature desorption techniques.

DISCUSSION AND CONCLUSIONS

These analyses permit us to generally characterize the relevant trapping parameters of the alloy system Fe-Ti-C, as summarized in Table VI. The implications of such trapping behavior will now be considered along with the limitations of the approaches used.

Our analysis of two of the trapping agents in Table VI, titanium substitutional atoms and TiC precipitates, has shown that they can effectively trap hydrogen in iron at room temperature, but in quite different ways. Titanium atoms or clusters of such are designated as reversible traps inasmuch as the occupancy time for a given hydrogen atom is short. Notwithstanding this, these reversible traps have a large effect on the effective diffusivity of hydrogen through iron, reducing it by an order of magnitude for an addition of 1.5 wt pct Ti. The interaction energy, E (Ti-H) $\approx$ 0.27 eV is of the same order as grain boundaries and dislocations, and, in fact, is similar to the interaction between nitrogen and vanadium[32] or titanium.[33] (This is in agreement with the fact that $e^{N}_{Ti} \cong e^{H}_{Ti}$.) We can thus successfully classify titanium as a medium-strength interstitial trap. Because it is homogeneously distributed throughout the lattice, it also provides a means of homogeneously distributing the interstitial species, in this case, hydrogen. This form of distribution reduces the susceptibility of these alloys to hydrogen-induced damage, by suppressing the formation of hydrogen-rich regions.[10,34] On the other hand, TiC precipitates particularly large ones,[10] are irreversible traps characterized by a large interaction energy, E(TiC-H), of 0.98 eV and consequently a long hydrogen residency time. As we have discussed,[10,34] these large, heterogeneously distributed traps promote hydrogen concentration centers and increase the alloy's susceptibility to hydrogen-induced damage.

The kinetics and trapping parameters of both kinds of these traps can be described in detail using metallography to obtain the number of each type of traps, and a theoretical and computer analysis fitting of the permeation transients[10-12] to obtain the kinetic parameters. Reversible trapping is analyzed from higher order transients (in our case the second and above) for which all the irreversible traps are filled. Irreversible trapping on the other hand is described with the first transient, where mixed trapping is occurring. The success of this study where for the first time the individual trapping parameters can be measured stems completely from our knowing both the species and number of the different trap types. When these are unknown or uncertain, the analysis suffers. For example, in some of the alloys localized regions of fine, coherent, TiC precipitates were found.[10] We could not fully characterize these, and the resultant observed discrepancies between the theory and the experimental results on irreversible trapping stemmed from the fact that coherent hydrogen traps are not as effective as incoherent ones.[37]

In summary, we present the following generalized method by which the trapping behavior of even more complex alloys can be obtained:

1) All potential hydrogen traps in the microstructure should be identified and analyzed as completely as possible using quantitative metallography.

2) The likelihood that such features could trap hydrogen should be tested by calculating or estimating the first-order interaction coefficients, most reliably for substitutional or interstitial solutes. For defects such as dislocations and precipitates, the attractive or repulsive nature of any interaction would probably have to be established experimentally, or from independent knowledge of the local stress field and the nature of any interfaces.

3) The trapping species of interest should be independently varied, and a series of successive permeation transients carried out. The transient for which reversible trapping dominates can be identified as that transient where the following linear relationship is obeyed:

$$D_o/D = 1 + b\,N_\gamma \qquad [27]$$

where N_γ is the number of suspected reversible traps. From the slope, b, all important reversible trapping parameters can be calculated (for example, these described by the McNabb-Foster model).

4) Irreversible trapping parameters are obtained by difference from the first transient where mixed trap-

ping occurs, and higher-order ones. This is possible because the final trapping capacities of each trap species are independent of one another.

5) It is anticipated, and supported by data,[10,34] that suitable choice of trap type and site is a highly practical means of developing alloys resistant to hydrogen embrittlement.

APPENDIX A: FREE ENERGIES FOR HYDRIDE FORMATION

Reaction Between Titanium and Hydrogen in Iron at Room Temperature

The free energy of the reaction in Eq. [2] is,

$$\Delta G = \Delta G^o + RT \ln Q.$$

i) Calculation of ΔG^o. Consider:

$Ti(s) + H_2(g)$	$= TiH_2(s)$	ΔG_1^o
$2\underline{H}$ (pct)	$= H_2(g)$	ΔG_2^o
$\underline{Ti}$ (pct)	$= Ti(s)$	ΔG_3^o
Ti (pct) $+ 2\underline{H}$ (pct)	$= TiH_2(s)$	ΔG^o

Note: $Ti(s)$ = Ti (solid)

$H_2(g)$ = H_2 (gas)

ΔG_1^o: Ref. A-1 gives: ΔG_1^o = 25.13 kcal/mole

ΔG_2^o: From Ref. A-2, the equilibrium wt pct of H in iron at room temperature is:

$$(\text{pct H}) = 5.4 \times 10^{-8}.$$

Since

$$H_2 = 2\underline{H} \text{ (pct)}$$

Then $\Delta G_2^o = RT \ln (\text{pct H})^2/pH_2$ with pH_2 = 1 atm. Then:

$$\Delta G_2^o = -19.82 \text{ kcal/mole}.$$

It can be shown that:[10]

$$\Delta G_3^o = RT \ln \frac{100\, M_{Ti}}{\gamma^o_{Ti}\, M_{Fe}} = 13.65 \text{ kcal/mole}$$

where:

$M_{Ti,Fe}$ = atomic mass of Ti and Fe.

and

$RT \ln \gamma^o_{Ti}$ = 11,000, in bcc Fe with bcc Ti as the standard state. (Ref. A-3)

Finally:

$$\Delta G^o = \Delta G_1^o + \Delta G_2^o + \Delta G_3^o = 31.3 \text{ kcal/mole}.$$

ii) Calculation of $RT \ln Q$. Consider that TiH_2 (s) has completely precipitated, then,

$$a_{TiH_2} = 1$$

so that:

$$RT \ln Q = RT\, n\, a_{\underline{Ti}}\, a^2_{\underline{H}} = RT \ln (\text{pct } \underline{Ti}) f_{\underline{Ti}} \times (\text{pct } \underline{H})^2 f_{\underline{H}}.$$

By expanding the activity coefficients in terms of their first order interaction coefficients (Eq. [1]) and using Table II values corrected to room temperature,[10,25] $RT \ln Q$ can be calculated for different values of (pct Ti) and (pct H).

We consider 3 values for the latter:

1) (pct $\underline{H}$) = 5.4×10^{-8}, which is the lowest equilibrium value.

2) (pct $\underline{H}$) = 1.18×10^{-5}, which is the value obtained from C_o, the concentration at steady state obtained for our permeation experiments for a current density of i = 0.8 mA/cm^2.

3) (pct $\underline{H}$) = 0.62×10^{-2}, supersaturation value obtained by considering 2 atoms of hydrogen for 1 atom of Ti in the alloy containing 0.15Ti. This value is 0.62×10^{-1} for 1.5Ti.

Note: Such a high concentration of hydrogen in Fe-Ti is obtainable when charging at high current density, in IN H_2SO_4 solution with a poison.

ΔG can then be calculated; the results are given in Table III (a). Similar calculations[10] yielded the results shown in Table III(b) and (c).

ACKNOWLEDGMENTS

This work was performed under the auspices and with the support of the Office of Naval Research under Contract N0014-75-C-0625, and constitutes part of a thesis submitted by G. M. Pressouyre for fulfillment of the requirements for a Ph.D. degree at Carnegie-Mellon University. We wish to thank Professor C. H. P. Lupis for valuable discussions concerning the thermodynamic calculations.

REFERENCES

1. L. S. Darken and R. P. Smith: *Corrosion*, 1949, vol. 5, p. 1.
2. A. J. Kumnick and H. H. Johnson: *Met. Trans.*, 1974, vol. 5, p. 1200.
3. J. P. Laurent, G. Lapasset, M. Aucouturier, and P. Lacombe: *Hydrogen in Metals*, I. M. Bernstein and A. W. Thompson, eds., p. 559, ASM, Ohio, 1974.
4. T. Asaoka: Thése Docteur-Ingénieur, Univ. Paris–Sud., 1976.
5. G. M. Evans and E. C. Rollason: *J. Iron Steel Inst.*, 1969, vol. 207, p. 1591.
6. D. M. Allen-Booth and J. Hewitt: *Acta Met.*, 1974, vol. 22, p. 171.
7. T. Boniszewski: Report P/10/66 of the British Welding Research Association, London, 1966.
8. A. W. Thompson and I. M. Bernstein: *Advance in Corrosion Science and Technology*, vol. 7, Plenum Press, New York, in press.
9. I. M. Bernstein, R. Garber, and G. M. Pressouyre: *Effect of Hydrogen on Behavior of Materials*, A. W. Thompson and I. M. Bernstein, eds., p. 37, TMS-AIME, New York, 1976.
10. G. M. Pressouyre: Ph.D. Thesis, Carnegie-Mellon University, 1977. Also issued on ONR Technical Report NR036-099-7.
11. A. McNabb and P. K. Foster: *Trans. TMS-AIME*, 1963, vol. 227, p. 618.
12. G. R. Caskey and W. L. Pillinger: *Met. Trans. A*, 1975, vol. 6A, p. 467.
13. R. A. Oriani: *Acta Met.*, 1970, vol. 18, p. 147.
14. M. Koiwa: *Acta Met.*, 1974, vol. 22, p. 1259.
15. G. M. Pressouyre and I. M. Bernstein: *Corrosion Sci.*, in press.
16. ASM Metals Handbook, vol. 8, 8th ed., 1973.
17. W. Tofaute and A. Buttinghaus: *Arch. Eisenhüettenw.*, 1938, vol. 12, p. 33.
18. P. B. Hirsch, A. Howie, R. B. Nicholson, D. W. Pashley, and M. J. Whelan: *Electron Microscopy of Thin Crystals*, Washington, Butterworths, 1965.
19. M. A. V. Devanathan and Z. O. J. Stachursky: *Proc. Roy. Soc.*, 1962, vol. A270, p. 90.
20. C. Wagner: *Thermodynamics of Alloys*, p. 47, Addison-Wesley, Reading, Mass., 1952.
21. C. H. P. Lupis and J. F. Elliott: *Acta Met.*, 1967, vol. 15, p. 265.
22. J. F. Elliott, M. Gleiser, and V. Ramakrishna: *Thermochemistry for Steelmaking*, Addison-Wesley, Reading, Mass., 1963.
23. G. K. Sigworth and J. F. Elliott: *Met. Sci. J.*, 1974, vol. 8, p. 298.
24. M. Weinstein and J. F. Elliott: *Trans. TMS-AIME*, 1963, vol. 227, p. 382.

25. C. H. P. Lupis and J. F. Elliott: *Acta Met.*, 1966, vol. 14, p. 529.
26. R. A. Oriani: Proceedings of Conference on Fundamental Aspects of Stress Corrosion Cracking, p. 32, R. W. Staehle, ed., Ohio State University, 1967.
27. J. Friedel: *Ber. der. Bunsen-Gesellschaft*, Bd. 76, 1972, vol. 8, p. 828.
28. J. Crank: *The Mathematics of Diffusion*, Clarendon Press, Oxford, 1956.
29. J. O'M. Bockris, M. A. Genshaw, and M. Fullenwider: *Electrochim. Acta*, 1970, vol. 15, p. 47.
30. W. Beck, J. O'M. Bockris, M. A. Genshaw, and P. K. Subramanyan: *Met. Trans.*, 1971, vol. 2, p. 883.
31. O. D. Gonzalez: *Trans. TMS-AIME*, 1969, vol. 245, p. 607.
32. A. J. Perry, M. Malone, and M. H. Boon: *J. Appl. Phys.*, 1966, vol. 37, p. 4705.
33. G. Szabó-Miszenti: *Acta Met.*, 1970, vol. 18, p. 477.
34. G. M. Pressouyre and I. M. Bernstein: *Abstract Bulletin of Conference on Residual Additives & Material Properties*, The Metals Society, London, 1978.
35. R. Gibala: *Trans. TMS-AIME*, 1967, vol. 239, p. 1574.
36. I. M. Bernstein: *Scr. Met.*, 1974, vol. 8, p. 343.
37. B. B. Rath and I. M. Bernstein: *Met. Trans.*, 1971, vol. 2, p. 2845.

APPENDIX REFERENCES

A-1. Janaf Thermochemical Tables, NSRDS-NBS37, Nat'l Bureau of Standards, 1971.
A-2. J. D. Fast: *Interaction of Metals and Gases*, vol. 1, Acad. Press, New York, 1965.
A-3. C. H. P. Lupis: Private Communication, Carnegie-Mellon Univ., Pittsburgh, 1977.